ANRIL is implicated in the regulation of nucleus and potential transcriptional target of E2F1

KAZUYUKI SATO[1], HIROKI NAKAGAWA[1], ATSUSHI TAJIMA[2], KENICHI YOSHIDA[1] and ITURO INOUE[2]

[1]Department of Life Sciences, School of Agriculture, Meiji University, Kawasaki; [2]Division of Molecular Life Science, School of Medicine, Tokai University, Isehara, Kanagawa, Japan

Received April 21, 2010; Accepted June 11, 2010

DOI: 10.3892/or_00000910

Abstract. *ANRIL*, a large antisense non-coding RNA, is in the proximity of *CDKN2A* and overlapped with *CDKN2B* at human chromosome 9p21, and has been strongly implicated in the association with high risk genetic markers of coronary artery disease (CAD). Mice model harboring large deletion of posterior part of *ANRIL* and CAD high risk genetic markers resulted in substantial suppression of both *CDKN2A* and *CDKN2B*; however, the mechanistic insights of regulation and function of *ANRIL* have remain elusive. To date multiple splice variants of *ANRIL* have been reported and expression of specific splice variant of *ANRIL* has been shown to be tightly associated with 9p21 CAD high risk markers. Here we identified a new splice variant of *ANRIL* and introduced it into HeLa cells to uncover functional aspects of *ANRIL* towards cellular function. For this purpose, we monitored global mRNA expressional changes and conducted gene ontology enrichment. The majority of mRNAs was down-regulated by *ANRIL* overexpression. Among them, a subset of mRNAs particularly involved in the regulation of nucleus and establishment or maintenance of chromatin architecture was significantly enriched. Such a circumstance was manifested after 48 h of *ANRIL* overexpression but no significant changes were seen after 24 h of *ANRIL* over-expression. Next we analyzed the sequences containing the intergenic region between *ANRIL* and *CDKN2A* (*p14ARF*) by introducing the sequences upstream of luciferase reporter gene. Based on the luciferase activity, the sequences tested were shown to act as promoter for *ANRIL* and *p14ARF*. Moreover, as well *p14ARF*, *ANRIL* promoter was responsive to transcription factor E2F1 in HeLa and A549 cells. Taken together, our present results indicate that co-regulation of *ANRIL* and *p14ARF* could be coupled by their unique intergenic region potentially through E2F1. Judged from the suppressive effect of *ANRIL* on a subset of mRNAs involved in the nuclear function suggests that *ANRIL* might have silencing effect on a specific gene set that accounts for a wide array of gene expression.

Correspondence to: Dr Kenichi Yoshida, Department of Life Sciences, School of Agriculture, Meiji University, 1-1-1 Higashimita, Tama-ku, Kawasaki, Kanagawa 214-8571, Japan
E-mail: yoshida@isc.meiji.ac.jp

Abbreviations: ANRIL, antisense non-coding RNA in the *INK4/ARF* locus; bp, base pairs; CAD, coronary artery disease; GAPDH, glyceraldehyde-3-phosphate dehydrogenase; GO, gene ontology; kb, kilobase; LD, linkage disequilibrium; PCR, polymerase chain reaction; RT, reverse transcription; SNP, single nucleotide polymorphism

Key words: ANRIL, *CDKN2A*, E2F1, nucleus, non-coding RNA

Introduction

The *INK4/ARF* locus at human chromosome 9p21 region has been implicated in tumorigenesis such as melanoma (1). The region harbors *CDKN2A* (*p16INK4a* and *p14ARF*; partially overlapped transcripts that use different reading frame by alternative promoter) and *CDKN2B* (*p15INK4b*), and these tumor suppressor genes have been shown to be frequently mutated, deleted or aberrantly methylated in various human cancer specimens (2,3). Modeling of such phenomena in mice has shown to be resulted in tumor-prone phenotype (4). Recently large antisense non-coding RNA in the *INK4/ARF* locus (*ANRIL*, alias *CDKN2BAS*) was found within the 403-kilobase (kb) germ line deletion of a French family with a history of melanoma and neural system tumors (5). Moreover, high susceptibility locus for coronary artery disease (CAD) in four European populations has been associated with haplo-type block spanning approximately 53-kb including the posterior part of *ANRIL* (6).

One common single nucleotide polymorphism (SNP) linked to atherosclerosis, which is used as a synonym of CAD, was mapped to linkage disequilibrium (LD) region overlapped with posterior part of *ANRIL*, and genotype associated with increased risk for CAD was shown to be strongly correlated with decreased expression level for *ANRIL*, *CDKN2A* and *CDKN2B* in peripheral blood T cells (7). In addition, based on five different microarray data, risk allele of one SNP located within 9p21 CAD risk locus has been shown to be associated with correlated expression pattern among *ANRIL*, *CDKN2A* and *CDKN2B*. Notably, within the same 9p21 CAD risk locus, conserved sequence has been shown to have enhancer activity by reporter gene assay (8). Moreover, homozygous risk allele within the conserved sequence has been revealed to be associated with the increased reporter activity, and also responsible

for expression pattern of *ANRIL* splice variants and *CDKN2B* expression level (8). Results from another study demonstrated that risk haplotype of 9p21 CAD locus selectively increased the expression level of specific *ANRIL* variant in peripheral blood mononuclear cells and this was directly related to the severity of atherosclerosis (9).

Recently solid evidence of a relationship between CAD-associated SNPs located within a 58-kb LD block on human chromosome 9p21 and expression level for neighboring genes was demonstrated by mouse model with targeted deletion of orthologous 70-kb non-coding interval on mouse chromosome 4 (10). In mice with 70-kb targeted deletion, cardiac expression of *Cdkn2a* and *Cdkn2b* were greatly suppressed, and expectedly, increased cell proliferation and deregulated senescence were observed (10). Collectively, the evidence suggests that *ANRIL* is involved in the regulation of neighboring genes such as *CDKN2A* and *CDKN2B*, and function of *ANRIL* is likely to be executed through co-regulated gene products; however, regulation and function of *ANRIL* is not yet fully understood.

Here we identified a novel splice variant of *ANRIL* and expressed it into HeLa cells. By conducting microarray and gene ontology enrichment analysis, we revealed that over-expression of *ANRIL* has a strong tendency to suppress mRNA expression particularly involving regulation of the nucleus. We also analyzed the sequences containing intergenic region of human *ANRIL* and *CDKN2A* (*p14ARF*), and to our knowledge, this is a first experimental demonstration that the sequences containing the intergenic region of *ANRIL* and *p14ARF* potentially is under control of cell cycle and the apoptosis regulator E2F1.

Materials and methods

Cells, plasmids and transfection. HeLa (cervical carcinoma) and A549 (lung adenocarcinoma) cells were cultured in Earle's modified Eagle's medium (Invitrogen, Carlsbad, CA) supplemented with 10% fetal bovine serum, 1% non-essential amino acids (Invitrogen) and antibiotic-antimycotics (Invitrogen). *Homo sapiens* cDNA clone L6ChoCKO-2-E10 5' (GenBank Accession No. CB109081) was provided by Functional Genomic Research Center, Korean Research Institute of Bioscience and Biotechnology. Cells were plated into 60 mm dishes 24 h prior to transfection and 2 μg of plasmid was transfected for *ANRIL* overexpression by using Lipofectamine Plus (Invitrogen) according to the manufacturer's instructions.

Promoter fragments were generated with the polymerase chain reaction (PCR) method from human genomic DNA (Promega, Madison, WI), and ligated into the respective enzyme *Kpn*I and *Hind*III sites of pGL3-Basic vector (Promega). PCR primers were designed on public genome sequence (GenBank No. AL449423) as follows (underlines indicate flanking enzyme site); *ANRIL*-851, GGGGTACCTG TGTGAAGGGAGGTCCAGG; *ANRIL*+29, CCCAAGCTTA GGGCCGTGTCAGGTGACG; *p14ARF*-388, GGGGTACC GGAATAGGGGAGCGGGGACG; *p14ARF*+22, CCC AAGCTTGCGCACCCGCCTTCCCTGAG, where minus position is relative to transcriptional start site as +1, which is identical to the 5'-end of *ANRIL* (GenBank Accession Version No. NR_003529.3) and *p14ARF* (GenBank Accession No. NM_058195), respectively. All the plasmid sequences were verified by sequencing at the Takara facility (Mie, Japan). In pGL3-*p14ARF* -388/+22, -175C was changed to -175T. pcDNA3 and pcDNA3-E2F1 has previously been described (11).

Luciferase reporter assay. For the promoter assay, $2x10^4$ cells were transfected with FuGene6 (Roche, Basel, Switzerland), in accordance with the manufacturer's instructions. Briefly, 200 ng of the expression plasmid, 200 ng of the firefly luciferase reporter plasmids pGL3-Basic (Promega) and 0.6 ng of the *Renilla* luciferase reporter plasmid pRL-TK (Promega) per 24-well dish were used for each transfection. Cells were lysed 24 h after transfection by applying 100 μl passive lysis buffer of the Dual Luciferase Reporter Assay kit (Promega) into each well of the 24-well plate. Five microliters of cell lysate was used for the luciferase reporter assay with the same kit according to the manufacturer's protocol. Light intensity was quantified in a GloMax 20/20n Luminometer (Promega). Experiments were performed at least in triplicate. As control for the transfection efficiency, the firefly luciferase activity values were normalized to the *Renilla* luciferase activity values. Data are presented as mean values ± SD. Statistical differences were analyzed using two-tailed Student's t-tests. A value of $P<0.05$ (n=3) was considered to indicate a statistically significant difference.

Real-time reverse transcription-PCR (RT-PCR). Total RNA (500 ng) was used for cDNA synthesis by PrimeScript RT (Takara, Otsu, Japan) with random 6-mers primer. SYBR Premix Ex Taq (Takara) was used for real-time PCR with primers in exons 17 and 18 (6). Glyceraldehyde-3-phosphate dehydrogenase (*GAPDH*) was detected and its mRNA level was used as a control.

Microarray analysis. Whole Human Genome oligoDNA microarray (Agilent Technologies, Santa Clara, CA; 4x44k platform) was used. Procedure for microarray analysis was performed according to manufacturer's standard protocol. Briefly, Cy3-labeled cRNA was synthesized by Low RNA Input Fluorescent Linear Amplification kit (Agilent). For data normalization, 75 percentile normalization using a per-chip 75 percentile of all measurements were performed. Duplicate and triplicate analyses were done for 24 and 48 h after transfection samples, respectively.

Results

Identification of a new splice variant of ANRIL and its effect on global gene signature. It has been shown that *ANRIL* gene spans ~130-kb and is consisted of 19 exons (5). *In silico* analysis has originally identified large (3834-bp, GenBank Accession No. DQ485453), which is considered as full-length and small (2659-bp, GenBank Accession No. DQ485454) *ANRIL* variants (5). We initially searched for other *ANRIL* splice variants in the public database. The sequence of L6ChoCKO-2-E10 5' (GenBank Accession No. CB109081) cDNA was identical to exon 1 and 5' part of exon 2 of *ANRIL*. Thus we determined the full-length sequence of the clone and revealed it encodes a new splice variant of *ANRIL* with

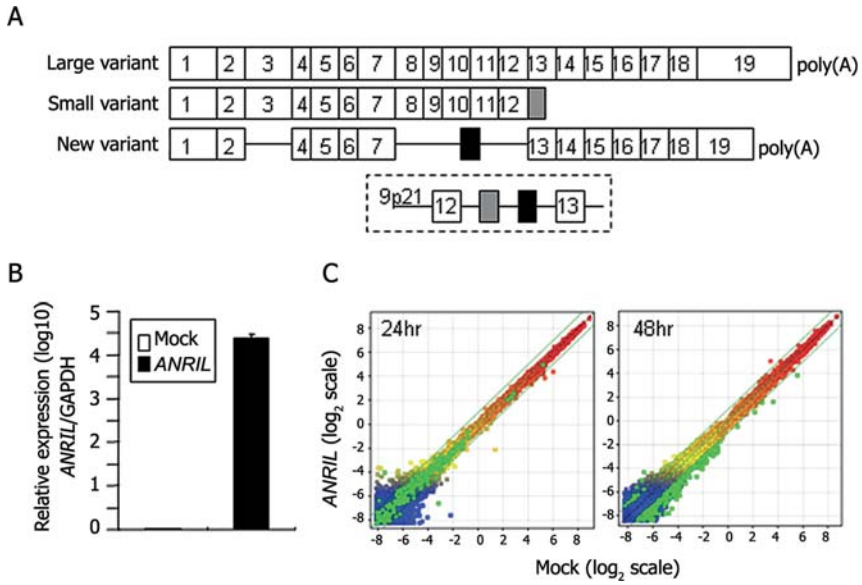

Figure 1. (A) Schematic representation of *ANRIL* splice variant. Large (DQ485453) and small (DQ485454) *ANRIL* variant (5) together with newly identified variant in this study (AB548314) are represented. Exons 1-19 are represented by boxes. Box with dotted lines indicates 9p21 genomic segment where intron 12 of *ANRIL* locus is shown. In it, grey and black box regions are alternatively spliced into small variant (end of exon 12) and new variant (between exons 7 and 13), respectively. (B) Real-time RT-PCR analysis of *ANRIL* expression in HeLa cells. After 48 h transfection, total RNA was extracted and used for real-time PCR. Relative expression level (log10) for *ANRIL/GAPDH* mRNA is indicated. (C) Scatter plot of 24 h (n=2) and 48 h (n=3) after *ANRIL* transfection compared to pcDNA3 control transfection in HeLa cells. Gene expression levels of *ANRIL* vs. control are shown as log2 scale: high-medium-low is represented by red-yellow-blue, respectively. Green spot represents *ANRIL*-regulated genes with 2-fold difference.

Table I. Top-five-ranked GO annotation affected by *ANRIL* overexpression.

GO accession	GO term	P-value	Count in selection	% Count in selection	Count in total	% Count in total
GO:0006325	Establishment or maintenance of chromatin architecture	0.0013	7	7.4	269	1.7
GO:0005634	Nucleus	0.0014	38	40.4	3992	25.8
GO:0051276| GO:0007001| GO:0051277	Chromosome organization and biogenesis	0.0052	7	7.4	347	2.2
GO:0008092	Cytoskeletal protein binding	0.0082	7	7.4	378	2.4
GO:0019219	Regulation of nucleobase, nucleoside, nucleotide and nucleic acid metabolic process	0.01	22	23.4	2175	14.1

Selection, 94 genes with GO annotation that showed expressional differences between control and *ANRIL* transfected HeLa cells. Total, 15448 genes with GO annotation that was used for GO enrichment analysis. Count, gene number included in GO accession. % Count, percentage of gene number included in selection or total. P-value, statistically significant difference of % count between selection and total.

poly(A), composed of exons 1, 2, 4-7, and alternatively spliced new exon located in intron 12, and 13-19 (Fig. 1A). The 2177-bp length new variant of *ANRIL* (GenBank Accession No. AB548314) has neither apparent open reading frames with longer size nor similarities with annotated proteins. This splice variant is different from previously reported 8 variants of *ANRIL* (12).

It has been widely recognized that non-coding RNAs are involved in the wide array of transcriptional networks (13). Therefore, we asked whether new splice variant of *ANRIL* has any effect on gene expression signatures. To accomplish this, we expressed *ANRIL* new splice variant into HeLa cells, and total RNAs were recovered for gene expression changes checked by microarray analysis. A new variant is originally cloned in pCNS-D2 that has CMV promoter up-stream of *ANRIL* cDNA. After 48 h of transfection, relative expression level of *ANRIL/GAPDH* mRNA was estimated over 10000-fold by real-time RT-PCR in *ANRIL*-transfected cells compared to control-transfected cells (Fig. 1B). Among 41035 transcripts, uniformly-detected 39859 transcripts were selected based on the criteria of per-prove CV (coefficient of variation) <50%. Next 248 transcripts were selected as they showed >2-fold changes and probability value (P-value) <0.05 (n=3) with no correction. They are shown as green spots in scatter plot as 235 mRNAs for down-regulated and 13 mRNAs for up-regulated in *ANRIL* overexpressed cells compared to

Table II. The genes annotated as GO term 'nucleus'.

GenBank/ Ensembl no.	Gene symbol	Description	Fold change	Regulation
NM_025114	CEP290	Centrosomal protein 290 kDa	7.96	Down
NM_001429	EP300	E1A binding protein p300	5.08	Down
NM_031283	TCF7L1	Transcription factor 7-like 1 (T-cell specific, HMG-box)	5.08	Down
AB040932	NPLOC4	KIAA1499	3.58	Down
NM_004241	JMJD1C	Jumonji domain containing 1C, transcript variant 2	3.49	Down
NM_007192	SUPT16H	Suppressor of Ty 16 homolog (*S. cerevisiae*)	3.48	Down
NM_005612	REST	RE1-silencing transcription factor	3.34	Down
NM_013275	ANKRD11	Ankyrin repeat domain 11	3.29	Down
NM_031407	HUWE1	HECT, UBA and WWE domain containing 1	3.09	Down
NM_015092	SMG1	PI-3-kinase-related kinase	2.85	Down
NM_014649	SAFB2	Scaffold attachment factor B2	2.79	Down
NM_003410	ZFX	Zinc finger protein, X-linked	2.72	Down
AK098787	PLEKHA2	FLJ25921, highly similar to tandem PH domain containing protein-2	2.59	Down
NM_033487	CDC2L1	Cycle 2-like 1 (PITSLRE proteins), transcript variant 3	2.55	Down
NM_015384	NIPBL	Nipped-B homolog (*Drosophila*), transcript variant B	2.53	Down
NM_018179	ATF7IP	Activating transcription factor 7 interacting protein	2.52	Down
NM_015029	POP1	Processing of precursor 1, ribonuclease P/MRP subunit (*S. cerevisiae*)	2.44	Down
BC011372	HIST1H2BN	Histone cluster 1, H2bn, with apparent retained intron	2.43	Down
NM_001620	AHNAK	AHNAK nucleoprotein (desmoyokin), transcript variant 1	2.42	Down
NM_017719	SNRK	SNF related kinase	2.39	Down
NM_003036	SKI	v-ski sarcoma viral oncogene homolog (avian)	2.39	Down
AF256215	ARNTL2	Cycle-like factor CLIF	2.38	Down
NM_014159	SETD2	SET domain containing 2	2.38	Down
ENST00000344293	TAF3	Transcription initiation factor TFIID subunit 3	2.37	Down
ENST00000255667	ANKRD32	Ankyrin repeat domain-containing protein 32	2.33	Down
NM_017643	MBTD1	mbt domain containing 1	2.32	Down
NM_006738	AKAP13	A kinase (PRKA) anchor protein 13, transcript variant 1	2.32	Down
NM_173215	NFAT5	Nuclear factor of activated T-cells 5, tonicity-responsive, transcript variant 5	2.25	Down
NM_018429	BDP1	B double prime 1, subunit of RNA polymerase III transcription initiation factor IIIB	2.25	Down
NM_021163	RBAK	RB-associated KRAB zinc finger	2.18	Down
NM_001008224	UACA	Uveal autoantigen with coiled-coil domains and ankyrin repeats, transcript variant 2	2.14	Down
NM_014562	OTX1	Orthodenticle homeobox 1	2.07	Down
NM_030751	ZEB1	Zinc finger E-box binding homeobox 1	2.04	Down
NM_006904	PRKDC	Protein kinase, DNA-activated, catalytic polypeptide, transcript variant 1	2.02	Down
NM_004852	ONECUT2	One cut domain, family member 2	2.01	Down
NM_004719	SFRS2IP	Splicing factor, arginine/serine-rich 2, interacting protein	2.01	Down
NM_002955	RREB1	Ras responsive element binding protein 1, transcript variant 2	2.27	Up
NM_014383	ZBTB32	Zinc finger and BTB domain containing 32	2.24	Up

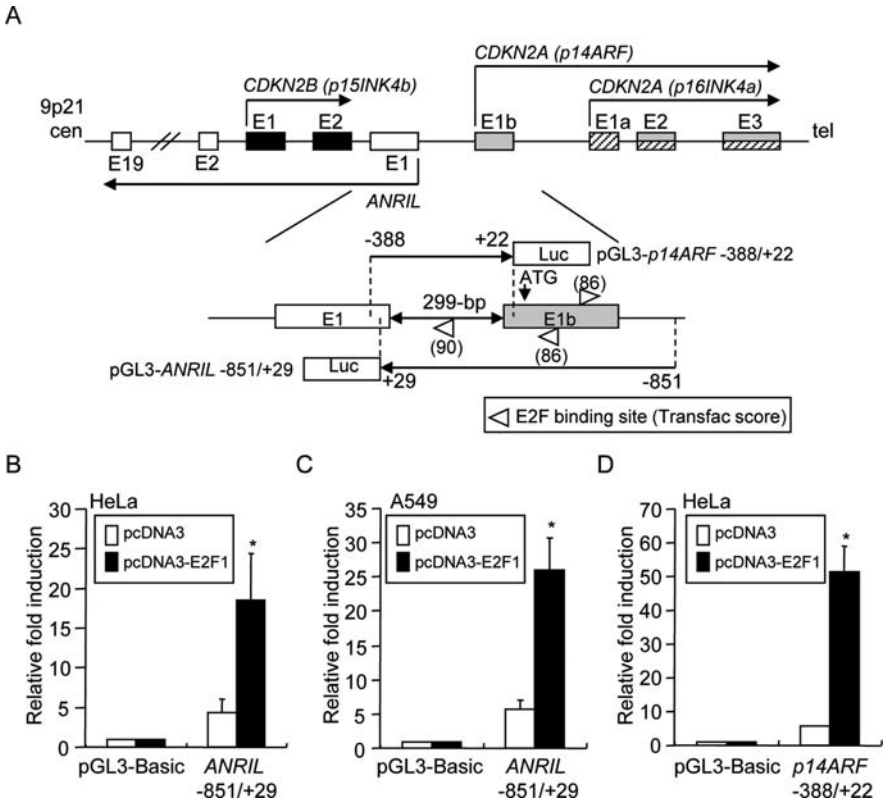

Figure 2. (A) Schematic representation of *ANRIL* and *p14ARF* intergenic region and their promoter constructs. The 9p21 genomic region containing exons of *CDKN2A* (*p14ARF* and *p16INK4a*), *CDKN2B* (*p15INK4b*) and *ANRIL* are shown. Both ends with centromere (cen) and telomere (tel) are indicated. The 299-bp intergenic region is indicated by two-headed arrow between exon 1 of *ANRIL* and exon 1ß of *p14ARF*. Down-pointing arrow indicates the position of translational initiation codon ATG of *p14ARF*. Regions indicated by directional line are used for luciferase (Luc) reporter assay. The nucleotide numbers represents relative position when +1 set as transcriptional start sites each for *ANRIL* and *p14ARF*, respectively. Triangular arrow indicates the position and direction of E2F binding site predicted by Transfac algorism (threshold >85). Basal and E2F1-regulated luciferase reporter activity of pGL3-*ANRIL* -851/+29 in HeLa (B), in A549 (C) cells and pGL3-*p14ARF* -388/+22 in HeLa (D) cells. Relative fold induction was shown as the value obtained by dividing luciferase activity of pGL3-*ANRIL* (or *p14ARF*) co-transfected with pcDNA3 or pcDNA3-E2F1 by that of pGL3-Basic co-transfected with pcDNA3 or pcDNA3-E2F1, respectively. White and black bars indicate pcDNA3 and pcDNA3-E2F1, respectively. Values are expressed as the means ± SD (n=3). *P<0.05 (compared with control pcDNA3-transfected cells), using a two-tailed Student's t-test.

control cells (Fig. 1C, right panel). In contrast to 48 h after *ANRIL* transfection, no significant changes (n=2) were observed after 24 h after *ANRIL* transfection (Fig. 1C, left panel). Expression levels for *CDKN2A* and *CDKN2B* were unchanged by *ANRIL* overexpression.

Subsequently gene ontology (GO) enrichment analysis was performed on GO annotation given genes (15448 out of 39859 and 94 out of 248 genes, respectively). Among the *ANRIL*-regulated mRNAs, GO terms with >5 gene numbers and P-value ≤0.01 were selected as top-five-ranked GO terms with low P-value (Table I). As top-ranked GO category, 7 out of 94 genes (count in selection) and 269 out of 15448 genes (count in total) were included in 'establishment or maintenance of chromatin architecture'. This means 7.4% (7/94) for % count in selection and 1.7% (269/15,448) for % count in total, respectively (Table I). Seven genes annotated as GO term 'establishment or maintenance of chromatin architecture' were all included in GO term 'nucleus'. Thirty-eight genes with GO term 'nucleus' were listed; 36 were down-regulated and 2 were up-regulated by *ANRIL* (Table II). Taken together, these results suggest that new splice variant of *ANRIL* has suppressive effect on genes involved in the regulation of nucleus and this effect could be maximized at 48 h after transfection in HeLa cells.

Characterization of intergenic region of ANRIL and CDKN2A by luciferase reporter assay. Pasmant *et al* have predicted that *ANRIL* and *p14ARF* may share a bidirectional promoter (5), but no experimental demonstration has been performed. Therefore, we attempted to analyze the promoter activity surrounding the intergenic region of *ANRIL* and *p14ARF*. For this purpose, we amplified the putative promoter region of *ANRIL* encompassing the -851 to +29 region (-851/ +29), in which the transcriptional start site of *ANRIL* was designated as +1, using PCR and then cloned it into a pGL3-Basic luciferase reporter plasmid (Fig. 2A). The amplified region contained three E2F binding sites, as predicted using Transfac software when the threshold was set to 85 (Fig. 2A). The pGL3-*ANRIL* -851/+29 reporter showed an ~4-fold induction of luciferase activity, compared with that in pGL3-Basic, in HeLa cells (Fig. 2B). Co-transfection of E2F1 with pGL3-*ANRIL* -851/+29 reporter showed an ~4-fold induction of luciferase activity, compared with that in pcDNA3 co-transfection, in HeLa cells (Fig. 2B). In A549 cells, almost the same basal promoter activity and E2F1 regulation was confirmed (Fig. 2C). An E2F binding site located within the intergenic region alone could be responsive to E2F1, indicating that one E2F binding site recognized in the intergenic region might have been bound by E2F1 (unpublished data).

The *p14ARF* promoter has been well characterized as E2F1-regulated gene promoter (14). As a positive control for E2F1-dependent promoter regulation, we constructed *p14ARF* promoter-luciferase reporter, named pGL3-*p14ARF* -388/+22 (Fig. 2A), and the basal promoter activity was ~5-fold, compared with that in pGL3-Basic and luciferase activity was ~9-fold up-regulated by E2F1 co-expression in HeLa cells (Fig. 2D). Collectively, these results demonstrated that the intergenic region could act as a bidirectional promoter and interactively regulated by E2F1 towards *ANRIL* and *p14ARF* gene direction.

Discussion

Implication of *ANRIL* in 9p21-associated human disease has been widely reported (5-10,12,15); however, any func-tional and mechanistic clues have yet to be determined largely due to non-coding feature of *ANRIL*. Here, we identified a new splice variant of *ANRIL* and introduced it into HeLa cells, and this resulted in a significant suppression of mRNAs involved in the regulation of nuclear function. Moreover, we constructed luciferase reporter for *ANRIL* promoter and revealed that *ANRIL* as well as *p14ARF* could be regulated by E2F1.

ANRIL and *p14ARF* are adjacent to each other and showed stronger similar expression pattern in normal human tissues and breast tumors compared to those of *p16INK4a* and *p15INK4b* (5). In the present study, we focused on *ANRIL* and *p14ARF* because the two genes are overlapped by just 299-bp. The intergenic region was proven to be a bidirectional promoter and co-regulated by E2F1. It has been shown that *p19ARF*, a mouse version of human *p14ARF*, is a direct transcriptional target of E2F1, and in turn, *p19ARF* (*p14ARF*) negatively regulate E2F1, thus forming a negative feedback loop (16-18). Based on the finding that *ANRIL* over-expression in HeLa cells led to the suppression of mRNAs involved in nuclear function, we tested whether *ANRIL* has any effect on E2F1- and p53-dependent transcriptional regulation, but no effect was found (unpublished data). Generally, promoters of long non-coding RNAs have been shown to be regulated by transcriptional factors such as Oct3/4, Nanog, CREB, Sp1, c-Myc, Sox2, NF-κB and p53 and marked with epigenetic histone modifications (19). Indeed, intergenic region between *ANRIL* and *p14ARF* was shown to be bound by CTCF, which possesses insulator and chromatin barrier activity, and CTCF activity and DNA methylation status were responsible for co-expression of *ANRIL* and *p14ARF* (20). Liu *et al* have reported that common allele of CAD susceptibility SNP that is approximately 120-kb distant from *ANRIL-p14ARF* intergenic region could affect the expression level of *ANRIL*, *p14ARF*, *p16INK4a* and *p15INK4b* in peripheral blood T cells (7). Therefore, our reporter plasmid could be useful to test whether enhancer sequences identified within 9p21 CAD susceptibility locus has synergistic effect on the promoter activity of *ANRIL-p14ARF* intergenic region.

The high-risk CAD haplotype has been shown to be associated with exons 13-19 of *ANRIL* (6,8). A new *ANRIL* variant used in this study also possesses exons 13-19, suggesting the new variant could represent high-risk CAD haplotype, but precise expression pattern of this new variant in cells or tissues affected by atherosclerosis should be further determined. Among *ANRIL*-regulated mRNAs, down-regulated mRNAs were majority compared to up-regulated mRNAs; however, our present results may represent a limited function of *ANRIL* variant because *ANRIL* has been shown to have multiple variants in tissue or cell-type specific manner (12). In addition, processing of *ANRIL* such as producing of mature microRNA and small peptide should be verified in a near future to fully understanding of molecular mechanism of *ANRIL*.

In conclusion, *ANRIL* and *CDKN2A* (*p14ARF*) are physically linked by the intergenic region and co-regulated by E2F1. The finding of suppressive effect of *ANRIL* on genes involved in the regulation of nuclear events could contribute to piece together details of *ANRIL* underlying human 9p21-associated pathogenesis.

Acknowledgements

We thank Kayo Yasuda and Hisako Kawata (Teaching and Research Support Center, Tokai University School of Medicine) for their technical assistance. This study was supported in part by Research Project Grant (B) by Institute of Science and Technology Meiji University (K.Y.), and 2009 Research and Study Program of Tokai University Educational System General Research Organization (A.T.).

References

1. Sharpless E and Chin L: The INK4a/ARF locus and melanoma. Oncogene 22: 3092-3098, 2003.
2. Gil J and Peters G: Regulation of the INK4b-ARF-INK4a tumour suppressor locus: all for one or one for all. Nat Rev Mol Cell Biol 7: 667-677, 2006.
3. Kim WY and Sharpless NE: The regulation of INK4/ARF in cancer and aging. Cell 127: 265-275, 2006.
4. Berger JH and Bardeesy N: Modeling INK4/ARF tumor suppression in the mouse. Curr Mol Med 7: 63-75, 2007.
5. Pasmant E, Laurendeau I, Héron D, Vidaud M, Vidaud D and Bièche I: Characterization of a germ-line deletion, including the entire INK4/ARF locus, in a melanoma-neural system tumor family: identification of ANRIL, an antisense non-coding RNA whose expression coclusters with ARF. Cancer Res 67: 3963-3969, 2007.
6. Broadbent HM, Peden JF, Lorkowski S, *et al*: Susceptibility to coronary artery disease and diabetes is encoded by distinct, tightly linked SNPs in the ANRIL locus on chromosome 9p. Hum Mol Genet 17: 806-814, 2008.
7. Liu Y, Sanoff HK, Cho H, *et al*: INK4/ARF transcript expression is associated with chromosome 9p21 variants linked to atherosclerosis. PLoS One 4: E5027, 2009.
8. Jarinova O, Stewart AF, Roberts R, *et al*: Functional analysis of the chromosome 9p21.3 coronary artery disease risk locus. Arterioscler Thromb Vasc Biol 29: 1671-1677, 2009.
9. Holdt LM, Beutner F, Scholz M, *et al*: ANRIL expression is associated with atherosclerosis risk at chromosome 9p21. Arterioscler Thromb Vasc Biol 30: 620-627, 2010.
10. Visel A, Zhu Y, May D, *et al*: Targeted deletion of the 9p21 non-coding coronary artery disease risk interval in mice. Nature 464: 409-412, 2010.
11. Yoshida K and Inoue I: Regulation of Geminin and Cdt1 expression by E2F transcription factors. Oncogene 23: 3802-3812, 2004.
12. Folkersen L, Kyriakou T, Goel A, *et al*: Relationship between CAD risk genotype in the chromosome 9p21 locus and gene expression. Identification of eight new ANRIL splice variants. PLoS One 4: E7677, 2009.
13. Mattick JS and Makunin IV: Non-coding RNA. Hum Mol Genet 15 Spec No 1: R17-R29, 2006.

14. Robertson KD and Jones PA: The human ARF cell cycle regulatory gene promoter is a CpG island which can be silenced by DNA methylation and down-regulated by wild-type p53. Mol Cell Biol 18: 6457-6473, 1998.
15. Schaefer AS, Richter GM, Groessner-Schreiber B, *et al*: Identification of a shared genetic susceptibility locus for coronary heart disease and periodontitis. PLoS Genet 5: E1000378, 2009.
16. Mason SL, Loughran O and La Thangue NB: p14(ARF) regulates E2F activity. Oncogene 21: 4220-4230, 2002.
17. Zhu JW, DeRyckere D, Li FX, Wan YY and DeGregori J: A role for E2F1 in the induction of ARF, p53 and apoptosis during thymic negative selection. Cell Growth Differ 10: 829-838, 1999.
18. Martelli F, Hamilton T, Silver DP, *et al*: p19ARF targets certain E2F species for degradation. Proc Natl Acad Sci USA 98: 4455-4460, 2001.
19. Taft RJ, Pang KC, Mercer TR, Dinger M and Mattick JS: Non-coding RNAs: regulators of disease. J Pathol 220: 126-139, 2010.
20. Rodriguez C, Borgel J, Court F, Cathala G, Forné T and Piette J: CTCF is a DNA methylation-sensitive positive regulator of the INK/ARF locus. Biochem Biophys Res Commun 392: 129-134, 2010.